

## ADAPTIVE BACKSTEPPING NONSINGULAR TERMINAL SLIDING MODE CONTROL OF SERVO SYSTEM BASED ON NEW SLIDING MODE AND REACHING LAW

QIXIN ZHU<sup>1,2,\*</sup>, JIAQI WANG<sup>1</sup> AND YONGHONG ZHU<sup>3</sup>

<sup>1</sup>School of Mechanical Engineering

<sup>2</sup>Key Laboratory of Intelligent Building Energy Efficiency  
Suzhou University of Science and Technology

No. 99, Xuefu Road, Huqiu District, Suzhou 215009, P. R. China  
1827325539@qq.com

\*Corresponding author: qxzhu@mail.usts.edu.cn

<sup>3</sup>School of Mechanical and Electronic Engineering  
Jingdezhen Ceramic Institute

Xianghu Town, Fuliang County, Jingdezhen 333001, P. R. China  
zhy\_patrick@163.com

Received April 2022; revised August 2022

**ABSTRACT.** *Aiming at the problem that the control accuracy of permanent magnet synchronous motor (PMSM) servo system is easily affected by parameter uncertainty, an adaptive backstepping nonlinear nonsingular terminal sliding mode control (ABNNTSMC) method is proposed in this paper. Based on the existing fast nonsingular terminal sliding mode, a new piecewise nonlinear nonsingular terminal sliding mode is proposed to improve the convergence speed and ensure the steady-state accuracy. At the same time, a new reaching law with attenuation term is proposed to reduce the vibration gradually. Finally, the adaptive law is used to estimate the moment of inertia and viscous friction coefficient of the system to improve the robustness of the system. Simulation results show that ABNNTSMC has higher steady-state accuracy and smaller vibration compared with several existing results.*

**Keywords:** Servo system, Sliding mode control, Backstepping control, Adaptive control, Reaching law

**1. Introduction.** Permanent magnet synchronous motor has the advantages of high-power density, high efficiency, high positioning accuracy, fast response speed, strong anti-interference ability and so on. Therefore, PMSM is widely used in electro-hydraulic servo system [1-3], industrial robot [4], military equipment [5], aerospace [6], computerized numerical control machine tools, XY axis platform and other high-precision automation equipment. However, at the same time, due to the influence of load disturbance, parameter changes, friction [7,8] and other uncertain factors, the control accuracy and tracking performance of PMSM will decline. Therefore, it is necessary to design a strong robust controller to effectively suppress the uncertainty, so as to improve the control performance of the servo system.

Sliding mode control has the advantages of good transient performance, insensitivity to parameter changes and strong robustness to disturbances. Therefore, it is widely used in real life, such as high-precision industrial production and processing, and electric vehicle [9]. The common sliding surfaces are linear sliding surface [10], integral sliding surface [11], fractional sliding surface [12] and terminal sliding surface. Among them, the biggest

advantage of the terminal sliding surface is that it can strictly prove the convergence time of the sliding surface, which provides a mathematical guarantee for the parameter tuning of the sliding surface. Then, with the continuous improvement of many scholars, the singular point problem of terminal sliding surface after derivation is solved, and further developed to fast nonsingular terminal sliding surface [13-15].

Besides the improvement of sliding surface, reaching law is also an important part of sliding mode control design. The design of reaching law not only determines the speed of the servo system converging to the sliding surface, but also affects the chattering. [6] showed that a new reaching law combines exponential reaching law and power reaching law, but the reaching speed of these reaching laws is only related to the value 's' of sliding mode, so that the amplitude of buffeting does not decrease with the decrease of state error. Therefore, the reaching law with attenuation term has become an important research direction in recent years. [16] showed that an improved adaptive variable rating exponential reaching law is proposed, which can shorten the time to reach the equilibrium point and reduce the chattering at the same time.

The advantage of backstepping control is that it can effectively deal with the nonlinear control problem of the system, adjust fewer parameters, and is easy to realize in engineering, so it has been widely valued by academia [17,18]. Finally, sliding mode control is combined with backstepping control in much literature. [1,2] showed that adaptive sliding mode backstepping control is introduced to electro-hydraulic servo system, which overcomes the nonlinear problem in complex system. [19] showed that adaptive radial basis function network based on sliding mode backstepping controller is introduced, which can overcome the uncertainty of the system.

Among the uncertainties of the system, the moment of inertia and viscous friction coefficient are the key factors to determine the control performance of the system. Among the traditional parameter identification methods, the common ones are sine signal integration method [20,21], steady-state direct method [22,23], least square method with forgetting factor [24], but they need to have specific conditions for speed and load torque. However, it is impossible for the system to keep in a specific motion condition all the time, so the adaptive identification algorithm will have more advantages [25-27].

The contribution of this paper is that based on the traditional nonsingular terminal sliding mode, a nonsingular terminal sliding mode with nonlinear switching term is proposed. When the error of the response curve is large, the starting speed of the sliding mode is faster. When the response curve approaches the given signal, the sliding mode can ensure higher steady-state accuracy. Then a reaching law with attenuation term is designed. When the error and the derivative of the error are large, the reaching speed can be accelerated. When the error is small, the attenuation term in the reaching law can further reduce the Buffeting. Finally, this paper combines sliding mode control with backstepping control, and introduces an adaptive identification algorithm of inertia moment and viscous friction coefficient to enhance the robustness of the control system and overcome the influence of parameter uncertainty on the system response.

The paper is organized in 5 sections including the introduction. Section 2 presents the design of sliding controller for PMSM. Section 3 presents the design of adaptive backstepping controller. Simulation is included to illustrate the results in Section 4. Section 5 summarizes this paper.

**2. Design of Sliding Mode Controller for PMSM.** The derivation of sliding mode control algorithm is based on the mathematical model of permanent magnet synchronous motor [27]. The  $d$ - $q$  models of motor in synchronous rotating coordinate system are expressed as follows.

$$\begin{cases} \dot{\theta} = \omega \\ \dot{\omega} = \frac{3P_n\Phi_f}{2J}i_q - \frac{B}{J}\omega \\ \dot{i}_d = -\frac{R}{L}i_d + P_n\omega i_q + \frac{1}{L}u_d \\ \dot{i}_q = -\frac{R}{L}i_q - P_n\omega i_d + \frac{1}{L}u_q - \frac{P_n\Phi_f}{L}\omega \end{cases} \quad (1)$$

where  $\theta$  is the rotation angle,  $\omega$  is the rotation speed,  $P_n$  is the pole pair number,  $\Phi_f$  is the permanent magnetic flux,  $J$  is the moment of inertia,  $B$  is the coefficient of viscosity,  $R$  is the stator resistance,  $L$  is the stator inductance,  $i_d, i_q$  is the  $d$ - $q$  axis stator current, and  $u_d, u_q$  is  $d$ - $q$  axis stator voltage.

Based on the above mathematical model, the step input signal is defined as  $\theta_d$  firstly, and then the tracking error  $e$  and the differential of tracking error  $\dot{e}$  are defined as follows:

$$e = \theta_d - \theta \quad (2)$$

$$\dot{e} = \dot{\theta}_d - \dot{\theta} = -\omega \quad (3)$$

[15] defined a nonsingular terminal sliding mode as follows:

$$s_1 = e + k_1|e|^\alpha \text{sgn}(e) + k_2|\dot{e}|^\beta \text{sgn}(\dot{e}) \quad (4)$$

where  $k_1, k_2$  are positive constants,  $1 < \beta < 2, \alpha > \beta$ ,  $\text{sgn}(\cdot)$  is the signum function.

This sliding mode has high convergence rate and can guarantee the convergence in finite time. However, when the system state is close to the equilibrium state, the convergence rate will decrease and the convergence accuracy is insufficient. In this paper, the sliding mode is improved as follows:

$$s_2 = ce + \dot{e} + k_1|e|^\alpha \text{sgn}(e) + k_2|\dot{e}|^\beta \text{sgn}(\dot{e}) \quad (5)$$

where  $c$  is the coefficient of linear part of sliding mode,  $c > 0$ .

The comparison of the response curves of the two sliding modes is shown in Figure 1.

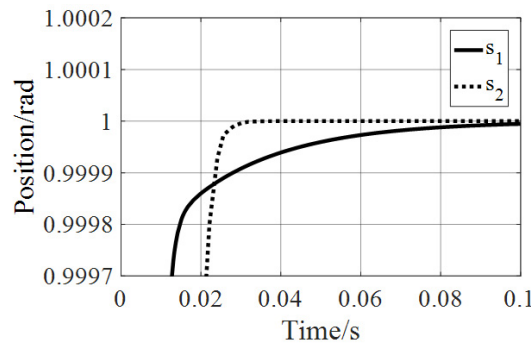


FIGURE 1. Comparison of two sliding modes

It can be seen from Figure 1 that the rising speed of  $s_1$  is faster than that of  $s_2$ , but the convergence accuracy of  $s_2$  is higher than that of  $s_1$ . Therefore, a new nonlinear switching sliding mode is proposed by combining the two sliding modes. When the error is large and the system state is far away from the equilibrium state, the  $s_1$  is adopted; when the error is small and the system state is close to the equilibrium state,  $s_2$  is adopted.

$$s = \begin{cases} e + k_{11}|e|^\alpha \text{sgn}(e) + k_{21}|\dot{e}|^\beta \text{sgn}(\dot{e}), & |e| > \delta \\ ce + \dot{e} + k_{12}|e|^\alpha \text{sgn}(e) + k_{22}|\dot{e}|^\beta \text{sgn}(\dot{e}), & |e| \leq \delta \end{cases} \quad (6)$$

where  $\delta$  is the error threshold of sliding mode switching.

After the sliding mode is designed, a new reaching law is improved based on the reaching law in [15] as follows,

$$\dot{s} = -ks - f(s) [\xi|\dot{e}|s + \eta\text{sat}(s)] \quad (7)$$

$$f(s) = \left( \frac{2}{1 + \exp(-as)} - 1 \right) \quad (8)$$

where  $k > 0$ ,  $\xi > 0$ ,  $\eta > 0$ ,  $a > 0$ . In the reaching law,  $-ks$  can accelerate the reaching speed when the system state is far away from the sliding mode, and reduce the reaching speed when the system state is close to the sliding mode. When the system is in the start-up phase,  $|\dot{e}|$  is larger. When the system response is close to the given signal, the errors  $e$  and  $|\dot{e}|$  are smaller. Therefore, the  $\xi|\dot{e}|s$  can ensure that the system has a larger reaching speed when it starts up. And when the system is close to the given signal, the  $\xi|\dot{e}|s$  can quickly reduce the reaching speed, so as to reduce the vibration. In order to further reduce the vibration caused by  $\xi|\dot{e}|s$  and  $\eta\text{sat}(s)$  after the system state reaches the sliding mode, a nonlinear function  $f(s)$  is multiplied before the two terms. When the system state is far away from the sliding mode,  $f(s)$  approaches to 1. When the system state reaches the sliding mode,  $f(s)$  approaches to 0, so vibration can be reduced.

After the reaching law is designed, the derivative of  $s$  is obtained and the saturation function  $\text{sat}(\cdot)$  is used to replace  $\text{sgn}(\cdot)$ . According to Equation (6), the actual derivative of  $s$  is as follows,

$$\dot{s} = \begin{cases} \dot{e} + k_{11}\dot{e}\alpha|e|^{\alpha-1} + k_{21}\ddot{e}\beta|\dot{e}|^{\beta-1}, & |e| > \delta \\ c\dot{e} + \ddot{e} + k_{12}\dot{e}\alpha|e|^{\alpha-1} + k_{22}\ddot{e}\beta|\dot{e}|^{\beta-1}, & |e| \leq \delta \end{cases} \quad (9)$$

In order to make the derivative of  $s$  meet the reaching law in Equation (7), Equation (9) can be made to be equal to Equation (7), and then the ideal second-order derivative of error  $\ddot{e}$  is shown as follows:

$$\ddot{e} = \begin{cases} \frac{-ks - f(s) [\xi|\dot{e}|s + \eta\text{sat}(s)] - \dot{e} - k_{11}\dot{e}\alpha|e|^{\alpha-1}}{k_{21}\beta|\dot{e}|^{\beta-1}}, & |e| > \delta \\ \frac{-ks - f(s) [\xi|\dot{e}|s + \eta\text{sat}(s)] - c\dot{e} - k_{12}\dot{e}\alpha|e|^{\alpha-1}}{1 + k_{22}\beta|\dot{e}|^{\beta-1}}, & |e| \leq \delta \end{cases} \quad (10)$$

According to Equation (1), Equation (3), the relationship between  $\dot{\omega}$  and  $\ddot{e}$ , and ideal current of  $q$ -axis  $i_q^*$  can be concluded as follows,

$$\dot{\omega} = \frac{3P_n\Phi_f}{2J}i_q - \frac{B}{J}\omega = -\ddot{e} \quad (11)$$

$$i_q^* = -\frac{2J}{3P_n\Phi_f}\ddot{e} + \frac{2B}{3P_n\Phi_f}\omega \quad (12)$$

According to the design of sliding mode controller in this chapter, the ideal  $q$ -axis current is obtained. In order to design a reasonable voltage value so that the actual current can accurately track the ideal current and overcome the influence of parameter uncertainty, an adaptive backstepping controller will be designed in Chapter 3.

**3. Design of Adaptive Backstepping Controller.** Backstepping controller is designed by introducing virtual state and virtual control function to ensure that the actual control quantity of each subsystem can approach the ideal control quantity, so as to achieve the purpose of system stability. According to Equation (12), the current errors of  $d$ - $q$  axis are defined as follows,

$$e_q = i_q^* - i_q, \quad e_d = i_d^* - i_d \quad (13)$$

The Lyapunov function  $V_1$  and the derivative of  $V_1$  are defined as follows,

$$V_1 = \frac{1}{2}s^2 + \frac{1}{2}e_q^2 + \frac{1}{2}e_d^2 \tag{14}$$

$$\dot{V}_1 = s\dot{s} + \dot{e}_q e_q + \dot{e}_d e_d = s\dot{s} - k_q^2 e_q^2 - k_d^2 e_d^2 < 0 \tag{15}$$

where  $k_q, k_d$  are positive constants.

According to Equation (1) and Equation (12),  $u_q$  and  $u_d$  can be concluded as follows,

$$\begin{cases} u_q = -\frac{2L}{3P_n\Phi_f} J \cdot \ddot{e} + \frac{2L}{3P_n\Phi_f} B\dot{\omega} + Ri_q + P_n\omega Li_d + P_n\Phi_f\omega + k_q^2 Le_q \\ u_d = Ri_d - P_n\omega Li_q + k_d^2 Le_d \end{cases} \tag{16}$$

In practical application, the uncertainty of system parameters will have an important impact on the control effect. In particular, the moment of inertia and friction viscosity coefficient will inevitably change in the long-term work. Therefore, this paper uses the adaptive algorithm to estimate the moment of inertia and viscous friction coefficient, and estimates  $J$  and  $B$  with  $\hat{J}$  and  $\hat{B}$ , to provide accurate parameters for the control variables. At this time, the control quantity  $u_q$  is as follows,

$$u_q = -\frac{2L}{3P_n\Phi_f} \hat{J} \cdot \ddot{e} + \frac{2L}{3P_n\Phi_f} \hat{B}\dot{\omega} + Ri_q + P_n\omega Li_d + P_n\Phi_f\omega + k_q^2 Le_q \tag{17}$$

Errors of the estimated  $\hat{J}$  and  $\hat{B}$  are defined as follows,

$$\tilde{J} = J - \hat{J}, \quad \tilde{B} = B - \hat{B} \tag{18}$$

Adaptive laws of  $\hat{J}$  and  $\hat{B}$  are defined as follows,

$$\begin{cases} \dot{\hat{J}} = -\frac{2\mu_1}{3P_n\Phi_f} \ddot{e}e_q \\ \dot{\hat{B}} = \frac{2\mu_2}{3P_n\Phi_f} \dot{\omega}e_q \end{cases} \tag{19}$$

where  $\mu_1, \mu_2$  are positive constants.

The Lyapunov function  $V_2$  is defined as follows,

$$V_2 = V_1 + \frac{1}{2\mu_1} \tilde{J}^2 + \frac{1}{2\mu_2} \tilde{B}^2 \tag{20}$$

Then, the result of the derivative of  $V_2$  is as follows,

$$\begin{aligned} \dot{V}_2 &= s\dot{s} - k_q^2 e_q^2 - k_d^2 e_d^2 - \frac{2}{3P_n\Phi_f} \ddot{e}e_q (J - \hat{J}) + \frac{2}{3P_n\Phi_f} \dot{\omega}e_q (B - \hat{B}) - \frac{1}{\mu_1} \dot{\tilde{J}}\tilde{J} - \frac{1}{\mu_2} \dot{\tilde{B}}\tilde{B} \\ \dot{V}_2 &= s\dot{s} - k_q^2 e_q^2 - k_d^2 e_d^2 - \left( \frac{2}{3P_n\Phi_f} \ddot{e}e_q + \frac{1}{\mu_1} \dot{\tilde{J}} \right) \tilde{J} + \left( \frac{2}{3P_n\Phi_f} \dot{\omega}e_q - \frac{1}{\mu_2} \dot{\tilde{B}} \right) \tilde{B} \\ \dot{V}_2 &= s\dot{s} - k_q^2 e_q^2 - k_d^2 e_d^2 < 0 \end{aligned} \tag{21}$$

According to Lyapunov stability theorem, the estimated value of system parameters will converge asymptotically, and the state of the system will converge to sliding surface. That is, even if the motor parameters are uncertain due to long-term operation, the state of the system can still ensure stable convergence and has strong robustness.

4. **Simulations.** The simulation model in this paper borrows the parameter data in [27]. As can be seen from Figure 2, there is a very close intersection between sliding surfaces  $s_1$  and  $s_2$ . The principle to select  $\delta$  is to be near the intersection and ensure that the overall sliding surface cannot have large speed change after switching and maintain smooth and continuous, so  $\delta$  is 0.12. According to the analysis, among the sliding surface parameters, the larger  $k_{11}$  and  $k_{12}$  are, the faster the starting speed is; the smaller  $k_{21}$  and  $k_{22}$  are, the faster the speed is, but they are prone to overshoot; the larger  $\alpha$  and  $\beta$  are, the slower the start-up speed is; the larger  $c$  is, the faster the start-up speed is. Among the reaching law parameters, the larger  $k$ ,  $\xi$  and  $\eta$  are, the faster the approaching speed is; the larger  $a$  is, the smaller the attenuation range of the attenuation term is, and the faster the attenuation speed of the approach law is. Therefore, under the condition of no overshooting vibration, the appropriate selection of parameters can meet the requirements of fast and stable response curve, as shown in Table 1.

According to the parameters in Table 1, the simulation model is built, as shown in Figure 2.

TABLE 1. Model parameters and controller parameters

Parameters	Value
Inertia ( $\text{kgm}^2$ )	$J = 0.001$
Viscosity coefficient ( $\text{Ns/rad}$ )	$B = 0.0001$
Stator resistance ( $\Omega$ )	$R = 2$
Stator inductance ( $\text{mH}$ )	$L = 6$
Pole pair	$P_n = 4$
Permanent magnetic flux ( $\text{Wb}$ )	$\Phi_f = 0.8$
Parameter of sliding surface	$k_{11} = 500$
Parameter of sliding surface	$k_{21} = 0.05$
Parameter of sliding surface	$\alpha = 2$
Parameter of sliding surface	$\beta = 5/3$
Parameter of sliding surface	$c = 500$
Parameter of sliding surface	$k_{12} = 10$
Parameter of sliding surface	$k_{22} = 0.1$
Parameter of reaching law	$k = 200$
Parameter of reaching law	$\xi = 10$
Parameter of reaching law	$\eta = 0.1$
Parameter of reaching law	$a = 10$
Error threshold of sliding mode switching	$\delta = 0.12$
Parameter of backstepping controller	$k_q = k_d = 100$
Parameter of adaptive controller	$\mu_1 = \mu_2 = 100$

In Figure 2  $k1\_1$ ,  $k2\_1$ ,  $k1\_2$  and  $k2\_2$  mean  $k_{11}$ ,  $k_{21}$ ,  $k_{12}$  and  $k_{22}$  respectively.  $de$  means the derivative of  $e$ ,  $d2e$  and  $d2e1$  all mean second-order derivative of error  $\ddot{e}$ .  $did$  and  $d iq$  mean the derivative of  $i_d$  and  $i_q$ , respectively.

The simulation time is set as 0.3 s, and the input signal is step signal. The ABNNTSMC proposed in this paper is compared with the adaptive nonsingular fast terminal sliding mode control (ANFTSMC) [15], adaptive linear sliding mode control (ALSMC) [5] and

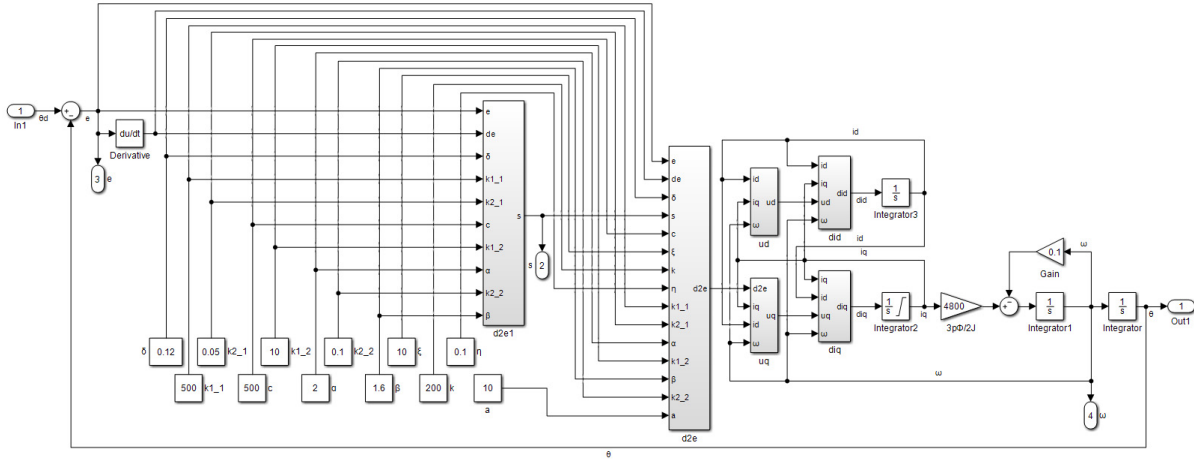


FIGURE 2. Structure diagram of simulation model for ABNNTSMC

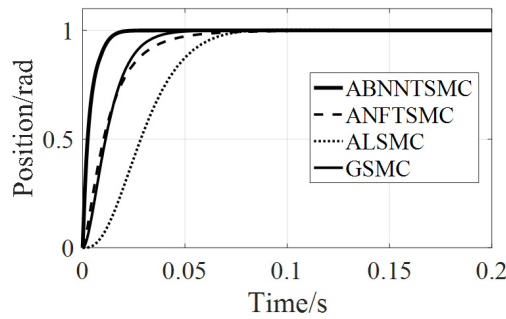
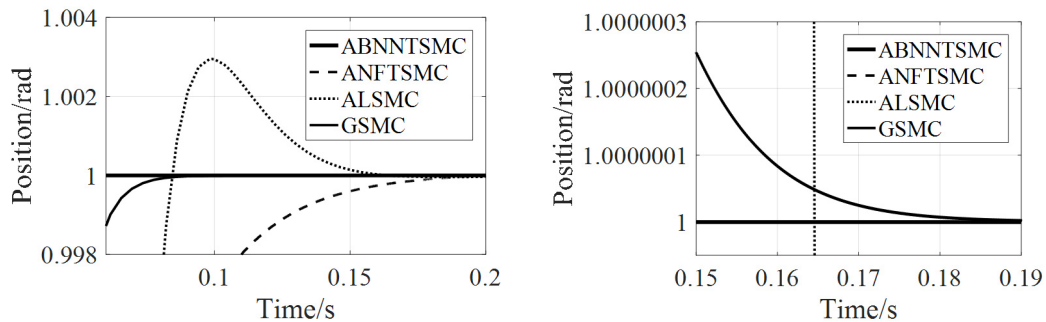


FIGURE 3. Comparison diagram of angle response tracking curve



(a) Comparison of all position response tracking curves

(b) Comparison of tracking curves of nonsingular terminal sliding mode angle response

FIGURE 4. Comparison diagram of local amplification of angle response tracking curve

global sliding mode control (GSMC) [11]. The simulation results are shown in Figures 3-7.

The comparison of simulation data of various sliding mode control is shown in Table 2.

As can be seen from Figure 3, ABNNTSMC has the strongest tracking performance and can track the input signal within 0.02 s. Moreover, there is no overshoot at all, because ABNNTSMC will switch to the sliding surface with small steady-state accuracy when it is close to the steady-state. However, the tracking performance of the other three methods is worse than ABNNTSMC. As can be seen from Figure 4(a), the response speed of

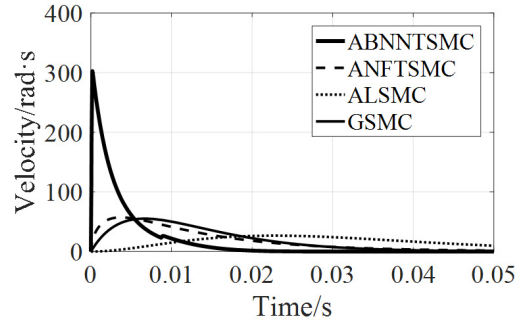


FIGURE 5. Comparison diagram of angular velocity response curves

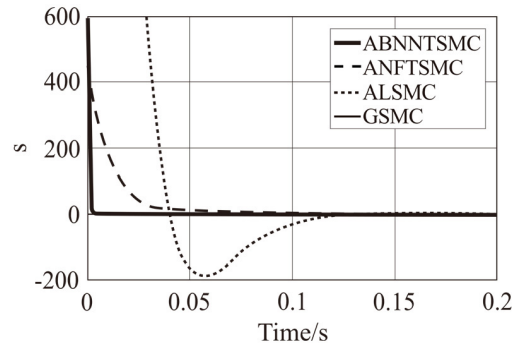


FIGURE 6. Comparison diagram of approaching effect of sliding mode

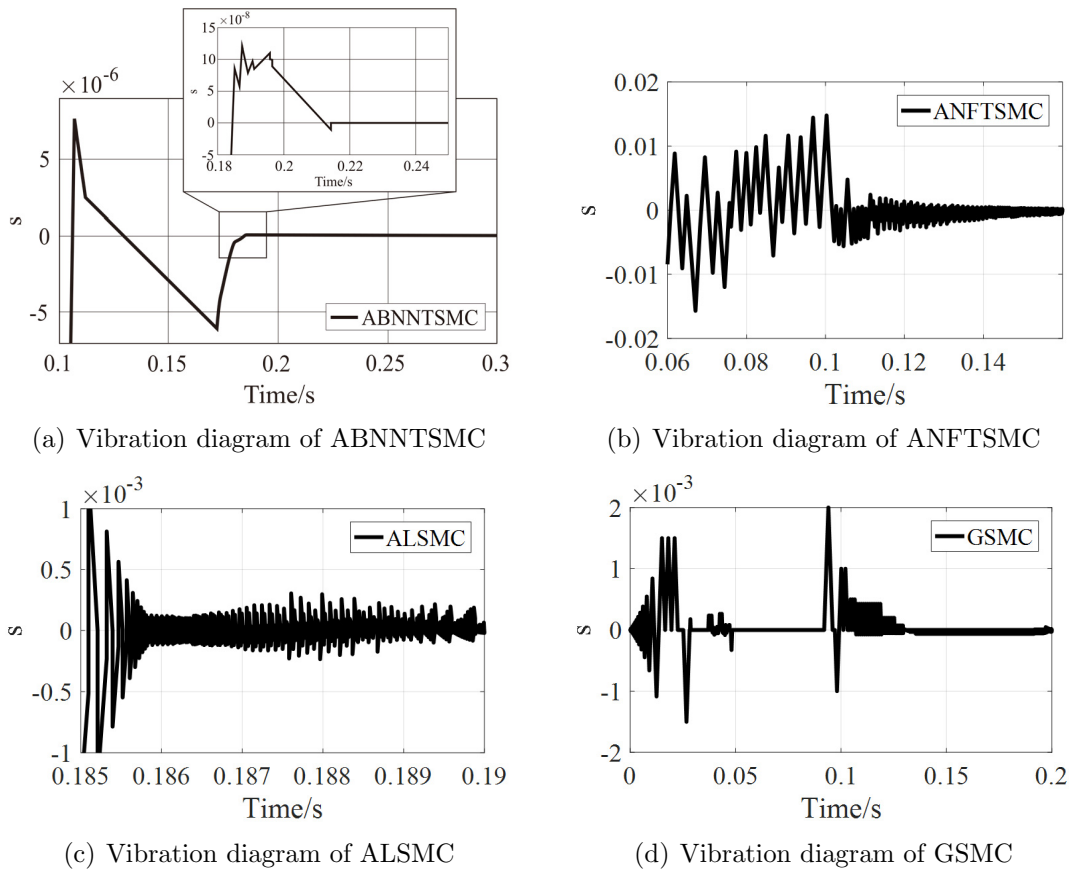


FIGURE 7. Vibration comparison diagram of sliding mode

TABLE 2. Comparison table of simulation data

	Tracking time	Maximum tracking speed	Arrival time of sliding surface	Vibration
ABNNTSMC	0.02 s	300 rad/s	0.005 s	The frequency is low and the amplitude decreases rapidly
ANFTSMC	0.14 s	57 rad/s	0.06 s	The frequency is high and the amplitude decreases gradually
ALSMC	0.08 s	27 rad/s	0.12 s	High frequency but no decrease in amplitude
GSMC	0.07 s	55 rad/s	0.002 s	High frequency and large amplitude variation

ANFTSMC and GSMC is slower than ABNNTSMC, and ALSMC has obvious overshoot. As can be seen from Figure 4(b), under the order of  $10^{-7}$  rad, GSMC has very small error, ALSMC has overshoot error and fluctuation change, and ANFTSMC is outside the image due to too large error. In comparison, ABNNTSMC still maintains high steady-state accuracy in Figure 4(b), and has the best response effect among the four sliding mode controls.

As can be seen from Figure 5, ABNNTSMC has the maximum rising speed, which can reach 300 rad/s. In addition, when ABNNTSMC completes the tracking of the input signal, the speed can quickly drop to 0 rad/s within 0.02 s, and the state is very stable. However, the rising speed of the other three methods is too slow, so it takes longer time to track the input signal, resulting in response lag. This shows that ABNNTSMC can not only achieve high tracking speed, but also be fast and stable after tracking.

As can be seen from Figure 6, GSMC belongs to the overall sliding surface, so the system state is on the sliding surface from the beginning. In addition to the other three sliding mode controls, ABNNTSMC can reach the sliding surface without overshoot in only 0.005 s. ANFTSMC can also reach the sliding surface in 0.06 s, but the reaching speed in the later stage is too slow. Although ALSMC reaches fast, it has serious overshoot and cannot meet the requirements of high precision. This indicates that ABNNTSMC has fast reaching speed and no overshoot. The reaching law proposed in this paper can meet higher tracking requirements.

As can be seen from Figure 7(a), the vibration frequency of ABNNTSMC is low, and the amplitude gradually decreases from  $10^{-6}$  rad to  $10^{-8}$  rad, and then decreases again. As can be seen from Figures 7(b)-7(d), the vibration frequencies of ANFTSMC, ALSMC and GSMC are very large, and the amplitude decreases slightly, but the order of magnitude is still  $10^{-3}$ . This shows that the reaching law proposed by ABNNTSMC has an obvious effect in restraining vibration.

**5. Conclusions.** For PMSM servo system, in order to improve the previous sliding mode control design, an adaptive backstepping nonlinear nonsingular terminal sliding mode control (ABNNTSMC) is proposed. The sliding mode is designed by switching two sliding modes. When the error is large, the sliding mode with faster speed is used. When the system is close to the stable state, the sliding mode with higher steady-state accuracy is switched. This sliding mode can not only accelerate the convergence speed, but also ensure higher steady-state accuracy. Then a new reaching law is designed, which can reach the sliding mode faster and suppress vibration gradually. Finally, the adaptive backstepping control for moment of inertia and viscous friction coefficient is designed to further enhance

the robustness in the case of parameter uncertainty. The simulation results show that the proposed method is feasible and practical.

However, the design of this paper is too complex, and there are some difficulties in the actual implementation. Moreover, there are fluctuations in the convergence process of parameter estimation, which has little impact on the overall response curve, but the optimal parameter estimation should be fast, stable and accurate. Therefore, the future research direction should be sliding mode controller with better effect and easier implementation, as well as more efficient parameter estimation.

**Acknowledgements.** This work is partially supported by the National Natural Science Foundation of China under Grant Nos. 51875380, 51375323 and 62063010, and Science and Technology Plan Project of Taizhou City under Grant No. TG202117.

## REFERENCES

- [1] D. T. Tran, D. X. Ba and K. K. Ahn, Adaptive backstepping sliding mode control for equilibrium position tracking of an electrohydraulic elastic manipulator, *IEEE Trans. Industrial Electronics*, vol.67, no.5, pp.3860-3869, 2020.
- [2] B. L. Hien, H. T. H. Thu and V. Q. Vinh, Dynamic surface control associates adapting external torque algorithm for electro-hydraulic velocity servo system, *International Organization of Scientific Research*, vol.10, no.5, pp.1-7, 2020.
- [3] X. Chen, D. Li, X. Yang and Y. Yu, Identification recurrent type 2 fuzzy wavelet neural network and L2-gain adaptive variable sliding mode robust control of electro-hydraulic servo system (EHSS), *Asian Journal of Control*, vol.20, no.4, pp.1480-1490, 2018.
- [4] X. Huang, Y. Wan, Y. Sun and J. Hou, Indirect adaptive fuzzy sliding-mode control for hydraulic manipulators, *Proc. of International Conference on Mechanical Design*, pp.229-242, 2020.
- [5] S. Nie, L. Qian, L. Tian and Q. Zou, Adaptive sliding mode control for electro-hydraulic position servo system of the elevation-balancing machine of artillery platform, *Proc. of IEEE Information Technology and Mechatronics Engineering Conference*, pp.731-735, 2018.
- [6] X. Zhang, H. Ma, Z. Li and W. Zao, An adaptive sliding mode controller with the exponential and power reaching law for discrete systems, *Proc. of Chinese Control Conference*, pp.2711-2716, 2018.
- [7] C. Wang and H. Zhao, Backstepping adaptive fuzzy control of servo system with LuGre friction, *MATEC Web of Conferences*, vol.104, pp.1-9, 2017.
- [8] F. Yue and X. Li, Robust adaptive integral backstepping control for opto-electronic tracking system based on modified lugre friction model, *ISA Transactions*, vol.80, pp.312-321, 2018.
- [9] J. S. V. Siva Kumar and P. Mallikarjuna Rao, Performance evaluation of sliding mode and linear quadratic regulator (LQR) control in interleaved double dual boost converter for electric vehicle applications, *ICIC Express Letters, Part B: Applications*, vol.11, no.8, pp.781-790, 2020.
- [10] M. Marcin, A. Lewicki and F. Wilczynski, Speed observer of induction machine based on backstepping and sliding mode for low-speed operation, *Asian Journal of Control*, vol.23, no.2, pp.636-647, 2021.
- [11] Y. Xin and X. Ping, Global robustness of sliding mode control for servo systems, *Proc. of Chinese Control and Decision Conference*, pp.667-671, 2018.
- [12] Y. Xie, X. Zhang, W. Meng et al., Coupled fractional-order sliding mode control and obstacle avoidance of a four-wheeled steerable mobile robot, *ISA Transactions*, vol.108, pp.282-294, 2021.
- [13] W. Zhu, X. Yang, F. Duan, Z. Zhu and B. Ju, Design and adaptive terminal sliding mode control of a fast tool servo system for diamond machining of freeform surfaces, *IEEE Trans. Industrial Electronics*, vol.66, no.6, pp.4912-4922, 2019.
- [14] D. Fu and X. Zhao, Adaptive backstepping global fast terminal sliding mode control for permanent magnet linear synchronous motor, *Transactions of China Electrotechnical Society*, vol.35, no.8, pp.1634-1641, 2020 (in Chinese).
- [15] D. Fu and X. Zhao, Adaptive nonsingular fast terminal sliding mode control for permanent magnet linear synchronous motor, *Transactions of China Electrotechnical Society*, vol.35, no.4, pp.717-723, 2020 (in Chinese).
- [16] Y. Cheng and J. Jiang, Study on control strategies for an antenna servo system on a carrier under large disturbance, *Transactions of the Institute of Measurement and Control*, vol.41, no.9, pp.2545-2554, 2019.

- [17] N. T. Thanh, P. N. Sam and D. P. Nam, An adaptive backstepping control for switched systems in presence of control input constraint, *Proc. of International Conference on System Science and Engineering*, pp.196-200, 2019.
- [18] J. Ting and D. Chen, Nonlinear backstepping control of SynRM drive systems using reformed recurrent Hermite polynomial neural networks with adaptive law and error estimated law, *Journal of Power Electronics*, vol.18, no.5, pp.1380-1397, 2018.
- [19] Z. Chen, Q. Gao and L. Tan, Adaptive backstepping sliding-mode control for permanent magnet linear synchronous motors, *Proc. of Chinese Control Conference*, pp.2690-2693, 2018.
- [20] M.-S. Yoo, S.-C. Choi, S.-W. Park and Y.-D. Yoon, Identification of mechanical parameters for position-controlled servo systems using sinusoidal commands, *Journal of Power Electronics*, vol.20, no.6, pp.1478-1487, 2020.
- [21] S. Kim, Moment of inertia and friction torque coefficient identification in a servo drive system, *IEEE Trans. Industrial Electronics*, vol.66, no.1, pp.60-70, 2019.
- [22] C. Lian, F. Xiao, S. Gao and J. Liu, Load torque and moment of inertia identification for permanent magnet synchronous motor drives based on sliding mode observer, *IEEE Trans. Power Electronics*, vol.34, no.6, pp.5675-5683, 2019.
- [23] F.-J. Lin, S.-G. Chen, S. Li, H.-T. Chou and J.-R. Lin, Online auto-tuning technique for IPMSM servo drive by intelligent identification of moment of inertia, *IEEE Trans. Industrial Informatics*, vol.16, no.12, pp.7579-7590, 2020.
- [24] F. Liu, E. Kang and N. Cui, Single-loop model prediction control of PMSM with moment of inertia identification, *IEEE Trans. Electrical and Electronic Engineering*, vol.15, no.4, pp.577-583, 2020.
- [25] L. Jiao, Y. Luo, P. Zhang, L. Li, X. Zheng, G. Qi, H. Jia and H. Liu, Design of the self-adaptive sliding mode position controller based on genetic algorithm optimization for the servo motor drive system, *Proc. of IEEE Information Technology and Mechatronics Engineering Conference*, pp.812-825, 2017.
- [26] X. Zhao, T. Wang and H. Jin, Intelligent second-order sliding mode control for permanent magnet linear synchronous motor servo systems with robust compensator, *IET Electric Power Applications*, vol.14, no.9, pp.1661-1671, 2020.
- [27] T. Du, C. Long, C. Jiang and J. Wang, Adaptive backstepping control of servo system based on load estimation, *Electric Drive*, vol.48, no.5, pp.49-52, 2018 (in Chinese).

## Author Biography



**Qixin Zhu** received his B.Sc. and M.Sc. degrees in Industrial Automation from Xi'an Polytechnic University, China, in 1994 and 1997, respectively. He received his Ph.D. degree in Control Theory and Control Engineering from Nanjing University of Aeronautics and Astronautics in 2003. He was with Nantong University, Nantong, China, from April 1997 to July 2004. He was with ASM Assembly Automation Ltd., Hong Kong, China, from July 2004 to August 2006. He was with East China Jiaotong University, Nanchang, China, from August 2006 to February 2013.

Prof. Zhu is currently a Professor at School of Mechanical Engineering, Suzhou University of Science and Technology, Suzhou, China. His research interests include servo control, networked control systems, robot, robust control and the applications of control theory in engineering. He has published over 100 papers in journals and conferences. He has actively served in a number of journals.



**Jiaqi Wang** received his B.Sc. degree in Mechanical and Electronic Engineering from Suzhou University of Science and Technology, China, in 2018; he received his M.Sc. degree in Mechanical Engineering from Suzhou University of Science and Technology, China, in 2022.

Mr. Wang's research interests include adaptive friction feedforward compensation, adaptive sliding mode backstepping control, filter vibration suppression and Smith prediction compensation.



**Yonghong Zhu** received his B.Sc. and M.Sc. degrees in Automation Engineering from Jiangxi Polytechnic University, Nanchang, China, in 1986 and 1989, respectively, and the Ph.D. degree in Control Theory and Control Engineering from Nanjing University of Aeronautics and Astronautics, Nanjing, China, in 2004.

Prof. Zhu is currently a Professor of Control Theory and Control Engineering at Jingdezhen Ceramic Institute, Jingdezhen, China. He has research interests in the areas of networked control systems, robust adaptive control, intelligent control, hybrid control and information fusion. He has published over 50 papers in journals and conferences.